97	EPHB4	7	NM_004444	c.C1096G	p.P366A	nonsynonymous SNV	-	-	-	-	-	-	-	-	-	-	-	-	-	-	○	-	-	-	-	-
98	ERBB2	17	NM_001005862	c.A3083C	p.D1028A	nonsynonymous SNV	○	-	○	○	○	○	-	-	○	-	-	○	○	-	-	○	○	○	○	-
99	ERN1	17	NM_001433	c.A2732G	p.Y911C	nonsynonymous SNV	-	-	○	-	-	-	-	-	-	-	-	-	-	-	-	-	-	-	-	-
100	ERN2	16	NM_033266	c.C314G	p.T105R	nonsynonymous SNV	-	-	-	-	-	-	-	-	-	-	-	-	○	-	-	-	-	-	-	-
101	FES	15	NM_001143784	c.G172A	p.G58S	nonsynonymous SNV	-	-	-	-	-	-	-	-	-	-	-	-	-	-	-	○	-	-	-	-
102	FLT3	13	NM_004119	c.C1295T	p.T432M	nonsynonymous SNV	-	-	-	-	-	-	-	-	-	-	-	-	○	-	-	-	-	-	-	-
103	GRK1	13	NM_002929	c.G880A	p.A294T	nonsynonymous SNV	-	-	-	○	-	-	-	-	-	-	-	-	-	-	-	-	-	-	-	-
104	GRK7	3	NM_139209	c.G1574C	p.G525A	nonsynonymous SNV	-	-	-	○	-	-	-	-	-	-	-	-	-	-	-	-	-	-	-	-
105	GSG2	17	NM_031965	c.T535A	p.S179T	nonsynonymous SNV	-	-	-	-	-	-	-	-	-	-	-	-	○	-	-	-	-	-	-	-
106	IKBKB	8	NM_001242778	c.C854T	p.T285M	nonsynonymous SNV	-	-	-	-	-	-	-	-	-	-	-	-	-	-	-	-	-	-	-	○
107	IRAK2	3	NM_001570	c.G1511A	p.R504Q	nonsynonymous SNV	-	-	-	-	-	-	-	-	○	-	-	-	-	-	-	-	-	-	-	-
108	IRAK4	12	NM_001145256	c.C134T	p.S45L	nonsynonymous SNV	-	○	-	-	-	-	-	-	-	-	-	-	-	-	-	-	-	-	-	-
109	KDR	4	NM_002253	c.C1325A	p.T442K	nonsynonymous SNV	-	-	-	-	-	-	-	-	-	-	-	-	-	-	○	-	-	-	-	-
110	KIAA1804	1	NM_032435	c.C2084T	p.A695V	nonsynonymous SNV	-	-	-	-	-	-	-	-	-	-	-	-	-	-	-	-	-	-	-	○
111	LATS1	6	NM_004690	c.G2984A	p.R995H	nonsynonymous SNV	-	-	-	-	○	-	-	-	-	-	-	-	-	-	-	-	-	-	-	-
112	LIMK1	7	NM_001204426	c.G1336A	p.G446R	nonsynonymous SNV	-	-	-	-	-	-	○	○	-	-	-	-	-	-	-	-	-	-	-	-
113	LRRK1	15	NM_024652	c.C2351A	p.S784Y	nonsynonymous SNV	-	-	-	○	-	-	-	-	-	-	-	-	-	-	-	-	-	-	-	-
114	LRRK2	12	NM_198578	c.G1901C	p.S634T	nonsynonymous SNV	○	-	-	-	-	-	-	-	-	-	-	-	-	-	-	-	-	-	-	-
115	MAP3K1	5	NM_005921	c.2953_2955del	p.985_985del	nonframeshift deletion	-	-	-	-	-	-	-	-	-	-	-	-	-	-	○	-	-	-	-	-
116	MAP3K12	12	NM_006301	c.C1789T	p.L597F	nonsynonymous SNV	-	-	-	-	-	-	-	-	-	-	-	-	-	-	-	○	-	-	-	-
117	MAP3K13	3	NM_001242314	c.G1810A	p.A604T	nonsynonymous SNV	-	-	-	-	-	-	-	-	-	-	-	-	○	-	-	-	-	-	-	-
118	MAP3K6	1	NM_004672	c.G2096A	p.R699H	nonsynonymous SNV	-	-	-	-	-	-	-	-	-	-	-	-	-	-	-	○	-	-	-	-
119	MAP3K7	6	NM_145332	c.T365G	p.L122W	nonsynonymous SNV	-	-	-	-	-	-	-	-	-	-	-	-	-	-	-	-	○	-	-	-
120	MAP4K3	2	NM_003618	c.C2314T	p.P772S	nonsynonymous SNV	-	-	-	-	-	-	○	○	-	-	-	-	-	-	-	-	-	-	-	-
121	MAP4K4	2	NM_145686	c.T1839G	p.S613R	nonsynonymous SNV	○	-	-	-	-	-	-	-	-	-	-	-	○	-	-	-	-	-	-	-
122	MAPK12	22	NM_002969	c.C902T	p.T301M	nonsynonymous SNV	-	-	-	-	-	-	-	-	-	-	-	-	-	-	-	-	○	-	-	-
123	MAPK4	18	NM_002747	c.A793C	p.S265R	nonsynonymous SNV	-	-	-	-	-	-	○	○	-	-	-	-	-	-	-	-	-	-	-	-
124	MAPK6	15	NM_002748	c.1687_1688del	p.563_563del	frameshift deletion	○	○	-	-	-	-	-	-	-	-	-	-	-	-	-	-	-	-	-	-
125	MAPKAPK2	1	NM_004759	c.A643C	p.T215P	nonsynonymous SNV	○	-	-	-	○	-	-	-	-	-	-	-	-	-	-	○	-	-	-	-
126	MARK1	1	NM_018650	c.T967C	p.Y323H	nonsynonymous SNV	-	-	-	-	-	-	-	-	-	-	-	-	-	-	○	-	-	-	-	-
127	MARK3	14	NM_001128920	c.G1139T	p.S380I	nonsynonymous SNV	-	-	○	-	-	-	-	-	-	-	-	-	-	-	-	-	-	-	-	-
128	MASTL	10	NM_032844	c.1011_1025del	p.337_342del	nonframeshift deletion	-	-	○	-	-	-	-	-	-	-	-	-	-	-	-	-	-	-	-	-
129	MERTK	2	NM_006343	c.T365C	p.I122T	nonsynonymous SNV	-	-	○	-	-	-	-	-	-	-	-	-	-	-	-	-	-	-	-	-
130	MOS	8	NM_005372	c.A373C	p.T125P	nonsynonymous SNV	-	-	-	-	-	-	-	-	-	-	-	-	○	-	-	-	-	-	-	-
131	MST1R	3	NM_002447	c.T2009G	p.V670G	nonsynonymous SNV	-	○	-	-	-	-	-	-	-	-	-	-	-	-	-	-	-	-	-	-
132	MYLK2	20	NM_033118	c.G1536T	p.E512D	nonsynonymous SNV	-	-	-	-	-	-	-	-	-	-	-	-	-	-	○	-	-	-	-	-
133	MYLK3	16	NM_182493	c.2129_2130insT	p.S710fs	frameshift insertion	-	-	-	-	-	-	-	-	-	-	-	-	○	-	-	-	-	-	-	-
134	MYLK4	6	NM_001012418	c.A943G	p.I315V	nonsynonymous SNV	-	-	○	-	-	-	-	-	-	-	-	-	-	-	-	-	-	-	-	-
135	MYO3A	10	NM_017433	c.A3552T	p.R1184S	nonsynonymous SNV	-	○	-	-	-	-	-	-	-	-	-	-	-	-	-	-	-	-	-	-
136	MYO3B	2	NM_001083615	c.G1097A	p.R366H	nonsynonymous SNV	-	-	-	-	○	-	-	-	-	-	-	-	-	-	-	-	-	-	-	-
137	NEK10	3	NM_199347	c.T494C	p.M165T	nonsynonymous SNV	-	○	-	-	-	-	-	-	-	-	-	-	-	-	-	-	-	-	-	-
138	NEK4	3	NM_003157	c.A296C	p.K99T	nonsynonymous SNV	-	-	-	-	-	-	-	-	-	-	-	-	-	-	-	-	○	-	-	-
139	NTRK3	15	NM_002530	c.T1230A	p.F410L	nonsynonymous SNV	-	-	-	-	-	-	-	-	-	-	-	-	-	-	-	○	-	-	-	-
140	NUAK1	12	NM_014840	c.G878T	p.R293L	nonsynonymous SNV	-	-	-	-	-	-	-	-	-	-	-	-	-	-	○	-	-	-	-	-
141	PDK2	17	NM_001199900	c.C526T	p.R176W	nonsynonymous SNV	-	-	-	-	-	-	-	-	-	○	-	-	-	-	-	-	-	-	-	-
142	PKN1	19	NM_002741	c.C83T	p.A28V	nonsynonymous SNV	-	-	○	-	-	-	-	-	-	-	-	-	-	-	-	-	-	-	-	-
143	PLK1	16	NM_005030	c.G671C	p.S224T	nonsynonymous SNV	-	○	-	-	-	-	-	-	-	-	-	-	-	-	-	-	-	-	-	-

144	PRKACB	1	NM_001242858	c.C738G	p.F246L	nonsynonymous SNV	-	-	-	-	-	-	-	-	-	-	-	-	-	-	○	-	-	-	-	-
145	PRKACG	9	NM_002732	c.G565A	p.A189T	nonsynonymous SNV	-	-	-	-	-	-	-	-	-	-	-	-	○	-	-	-	-	-	-	-
146	PRKCQ	10	NM_006257	c.A428G	p.H143R	nonsynonymous SNV	-	-	-	-	-	○	-	-	-	-	-	-	-	-	-	-	-	-	-	-
147	PRKCZ	1	NM_002744	c.A295C	p.T99P	nonsynonymous SNV	-	-	-	-	-	-	-	○	-	-	-	-	-	-	-	-	○	-	-	-
148	PTK2	8	NM_153831	c.3127_3131del	p.1043_1044del	frameshift deletion	-	-	-	-	-	○	-	-	-	-	-	-	-	-	-	-	-	-	-	-
149	RET	10	NM_020630	c.G1588A	p.E530K	nonsynonymous SNV	-	○	-	-	-	-	-	-	-	-	-	-	-	-	-	-	-	-	-	-
150	RIPK4	21	NM_020639	c.C2296G	p.L766V	nonsynonymous SNV	-	-	-	-	-	-	-	-	-	-	-	-	○	-	-	-	-	-	-	-
151	RNASEL	1	NM_021133	c.G1823A	p.R608Q	nonsynonymous SNV	-	-	○	-	-	-	-	-	-	-	-	-	-	-	-	-	-	-	-	-
152	RPS6KA1	1	NM_002953	c.T214G	p.S72A	nonsynonymous SNV	-	-	○	-	-	-	-	-	-	-	-	-	-	-	-	-	-	-	-	-
153	RPS6KB2	11	NM_003952	c.G1264A	p.V422I	nonsynonymous SNV	-	○	-	-	-	-	-	-	-	-	-	-	-	-	-	-	-	-	-	-
154	RPS6KC1	1	NM_001136138	c.A2204G	p.K735R	nonsynonymous SNV	-	-	-	-	-	-	-	-	○	-	-	-	-	-	-	-	-	-	-	-
155	SCYL1	11	NM_001048218	c.G163A	p.E55K	nonsynonymous SNV	-	-	○	-	-	-	-	-	-	-	-	-	-	-	-	-	-	-	-	-
156	SCYL2	12	NM_017988	c.T767C	p.M256T	nonsynonymous SNV	-	-	-	-	-	-	-	-	-	○	-	-	-	-	-	-	-	-	-	-
157	SGK2	20	NM_016276	c.A923C	p.H308P	nonsynonymous SNV	-	○	-	-	-	○	○	○	-	○	○	-	-	○	○	○	-	-	-	○
158	SIK1	21	NM_173354	c.G1888A	p.A630T	nonsynonymous SNV	-	-	-	-	-	-	-	-	-	-	-	-	○	-	-	-	-	-	-	-
159	SRPK1	6	NM_003137	c.G1427A	p.G476E	nonsynonymous SNV	-	-	○	-	-	-	-	-	-	-	-	-	-	-	-	-	-	-	-	-
160	STK10	5	NM_005990	c.G2753A	p.R918Q	nonsynonymous SNV	-	-	-	-	-	-	-	-	-	-	-	-	-	-	-	○	-	-	-	-
161	STK17B	2	NM_004226	c.A304T	p.N102Y	nonsynonymous SNV	○	-	-	-	-	-	-	-	-	-	-	-	-	-	-	-	-	-	-	-
162	STK24	13	NM_003576	c.G310A	p.D104N	nonsynonymous SNV	-	-	-	-	-	-	-	-	-	-	-	○	-	-	-	-	-	-	-	-
163	STK4	20	NM_006282	c.G350A	p.R117Q	nonsynonymous SNV	-	-	-	-	-	-	-	-	-	○	-	-	-	-	-	-	-	-	-	-
164	STK40	1	NM_032017	c.769_770del	p.257_257del	frameshift deletion	-	-	-	-	-	-	-	-	-	-	-	-	○	-	-	-	-	-	-	-
165	STYK1	12	NM_018423	c.A91G	p.T31A	nonsynonymous SNV	-	-	-	-	-	-	-	-	-	-	-	-	-	-	○	-	-	-	-	-
166	TBCK	4	NM_001163435	c.G19A	p.A7T	nonsynonymous SNV	-	-	○	-	-	-	-	-	-	-	-	-	-	-	-	-	-	-	-	-
167	TEK	9	NM_000459	c.A880G	p.K294E	nonsynonymous SNV	○	○	○	○	○	○	○	-	○	-	-	○	-	-	-	-	○	○	○	-
168	TEX14	17	NM_031272	c.G3570C	p.Q1190H	nonsynonymous SNV	-	-	-	-	-	-	-	-	-	-	-	-	-	-	○	-	-	-	-	-
169	TGFBR1	9	NM_001130916	c.G856C	p.D286H	nonsynonymous SNV	-	-	-	-	-	-	-	-	-	-	-	-	-	-	-	-	○	-	-	-
170	TNK2	3	NM_001010938	c.C1814T	p.P605L	nonsynonymous SNV	-	-	-	-	-	-	-	-	-	-	-	-	-	-	○	-	-	-	-	-
171	TRIB2	2	NM_021643	c.A494C	p.H165P	nonsynonymous SNV	-	-	-	-	-	-	-	-	-	-	-	-	○	-	-	-	-	-	-	-
172	TRIM28	19	NM_005762	c.C2441T	p.P814L	nonsynonymous SNV	-	-	-	-	-	-	-	-	-	-	-	○	-	-	-	-	-	-	-	-
173	TRIO	5	NM_007118	c.T7775C	p.F2592S	nonsynonymous SNV	-	-	○	-	○	-	-	-	-	-	-	-	-	-	-	○	-	○	-	-
174	TRPM6	9	NM_001177310	c.C3733A	p.P1245T	nonsynonymous SNV	-	-	-	-	-	-	-	-	-	-	-	-	-	-	-	-	-	-	-	○
175	TSSK4	14	NM_174944	c.T311A	p.L104Q	nonsynonymous SNV	-	-	-	-	-	○	-	-	-	-	-	-	-	-	-	-	-	-	-	-
176	TTBK1	6	NM_032538	c.A295G	p.N99D	nonsynonymous SNV	-	-	-	-	○	-	-	-	-	-	-	-	-	-	-	○	-	-	-	-
177	TYK2	19	NM_003331	c.1036_1037insG	p.N346fs	frameshift insertion	○	○	-	○	○	-	-	○	-	-	○	○	○	-	○	-	○	-	○	-
178	TYRO3	15	NM_006293	c.G1135A	p.A379T	nonsynonymous SNV	-	-	-	-	-	-	-	-	-	-	-	-	-	-	-	-	-	○	-	-
179	UHMK1	1	NM_175866	c.C29T	p.A10V	nonsynonymous SNV	-	-	-	-	-	-	-	-	-	-	-	-	-	-	-	○	-	-	-	-
180	ULK2	17	NM_014683	c.2621delA	p.Q874fs	frameshift deletion	-	-	-	-	-	-	-	-	-	-	-	-	-	-	-	○	-	-	-	-
181	ULK4	3	NM_017886	c.G3746A	p.R1249Q	nonsynonymous SNV	-	-	-	-	-	-	-	-	-	-	-	-	-	-	-	-	-	-	-	○
182	VRK2	2	NM_001130481	c.G775A	p.A259T	nonsynonymous SNV	-	-	-	-	-	-	-	-	-	-	-	○	-	-	-	-	-	-	-	-
183	WNK1	12	NM_014823	c.C4468G	p.P1490A	nonsynonymous SNV	-	-	-	-	-	-	-	-	-	-	-	-	-	-	-	-	-	-	-	○
184	WNK2	9	NM_006648	c.G5350A	p.V1784M	nonsynonymous SNV	-	-	-	-	-	-	-	-	-	○	-	-	-	-	-	-	-	-	-	-
185	WNK4	17	NM_032387	c.G2167A	p.E723K	nonsynonymous SNV	-	-	-	-	-	-	-	-	-	-	-	-	-	-	-	-	-	-	○	-
186	YES1	18	NM_005433	c.G271C	p.G91R	nonsynonymous SNV	-	-	-	-	○	-	-	-	-	-	-	-	-	-	-	-	-	-	-	-

[a]The 20 HCC cell lines analyzed were SNU-449, HUH-6, JHH-7, SK-Hep1, JHH-5, C3A, HepG2, JHH-4, huH-1, HLE, SNU-398, SNU-475, HLF, Alexander, KIM-1, JHH-1, JHh-2, SNU-182, SNU-423 and SNU-387.
[b]RefSeq Accession number registered in the National Center for Biotechnology Information (NCBI) database (http://www.ncbi.nlm.nih.gov/sites/entrez?db=gene).
Abbreviation: Chr, chromosome

Supplementary Table S7.
mTOR and MAPK pathway gene alterations in the HCC cell lines

Gene symbol	Alternative name	rsID[a]	RefSeq ID[b]	Chr	Genome position	cDNA	Amino acid	Cell lines																		
								SNU44	HUH6	JHH7	HuH7	SKHep1	JHH5	C3A	HepG2	JHH4	huH1	HLE	SNU39	SNU47	HLF	Alex	KIM1	JHH1	SNU18	SNU42	SNU378
BRAF		rs113488022	NM_004333	7	140453136	c.T1799A	p.V600E	–	–	–	–	O	–	–	–	–	–	–	–	–	–	–	–	–	–	–	–
RPS6KA1	RSK1		NM_002953	1	26873463	c.T214G	p.S72A	–	–	O	–	–	–	–	–	–	–	–	–	–	–	–	–	–	–	–	–
RPS6KA1	RSK1	rs2229712	NM_002953	1	26883511	c.A1004C	p.K335T	–	–	–	–	–	–	–	–	–	O	–	–	O	–	–	–	–	O	–	–
RPS6KA6	RSK4	rs6616890	NM_014496	X	83320017	c.G2074A	p.D692N	O	–	–	–	–	–	–	–	–	–	–	O	O	–	–	O	–	–	–	–
RPS6KB2	S6K2		NM_003952	11	67202161	c.G1264A	p.V422I	–	O	–	–	–	–	–	–	–	–	–	–	–	–	–	–	–	–	–	–
RPS6KB2	S6K2	rs55987642	NM_003952	11	67200812	c.C800T	p.P267L	–	–	–	–	O	–	–	–	O	–	–	–	–	–	–	O	O	–	–	–
RPS6KB2	S6K2	rs13859	NM_003952	11	67202156	c.C1259T	p.A420V	O	O	O	O	O	–	–	–	O	O	–	–	–	–	O	O	O	O	–	–
STK11	LKB1	rs59912467	NM_000455	19	1223125	c.C1062G	p.F354L	–	–	O	–	–	–	–	–	–	–	–	–	O	–	–	–	–	–	–	–

[a]Reference Cluster ID registered in the dbSNP (http://www.ncbi.nlm.nih.gov/projects/SNP/) database (as of March 2013).
[b]RefSeq accession number registered in the NCBI database.
Shaded rows indicate DNA variations not registered as genetic polymorphisms in the dbSNP database.

Supplementary Table S8. Chou-Talalay median dose effect analysis

	1	2	3	4	5
AZD8055 (nM)	**12.5**	**25**	**50**	**100**	**200**
CI-1040 (μM)	**3.75**	**7.5**	**15**	**30**	**60**
Drug Combination Ratio	**1:300**	**1:300**	**1:300**	**1:300**	**1:300**
CI[a]	**0.893**	**0.766**	**0.711**	**0.709**	**0.835**

[a]CI value was calcurated using the CompuSyn software package (ComboSyn, Inc, http://www.combosyn.com). CI = 1, additive effect; CI <1, synergistic effct; CI >1, antagonistic effect.
Abbreviations: CI, combination index.

Supplementary Table S9. List of the MAPK and mTOR signaling components for unsupervised hierarchical clustering analyses

#	Signaling Components	Phosphorylation site(s)	KEGG Pathway[a]	CST Antibody Category
1	p-p53	Ser20	MAPK	DNA damage
2	p-p53	Ser46	MAPK	DNA damage
3	p-p53	Ser15 16G8	MAPK	DNA damage
4	p-p53	Ser37	MAPK	DNA damage
5	p-p53	Ser392	MAPK	DNA damage
6	p-p53	Ser6	MAPK	DNA damage
7	p-p53	Ser9	MAPK	DNA damage
8	p-p53	Ser15	MAPK	DNA damage
9	p-NFkB p65	Ser536	MAPK	NFkB
10	p-NFkB p65	Ser276	MAPK	NFkB
11	p-NFkB p65	Ser468	MAPK	NFkB
12	p-ATF-2	Thr71 11G2	MAPK	p38 MAPK
13	p-HSP27	Ser82	MAPK	p38 MAPK
14	p-MAPKAPK-2	Thr222	MAPK	p38 MAPK
15	p-MAPKAPK-2	Thr2334	MAPK	p38 MAPK
16	p-MKK3/MKK6	Ser189/207	MAPK	p38 MAPK
17	p-MSK1	Thr581	MAPK	p38 MAPK
18	p-p38 MAPK	Thr180/Y182	MAPK	p38 MAPK
19	p44/42 MAP kinase	Thr202/Tyr204	MAPK	Ras-Raf
20	p-CREB	Ser133	MAPK	Ras-Raf
21	p-MEK1/2	Ser217/221	MAPK	Ras-Raf
22	p-Mnk1	Thr197/202	MAPK	Ras-Raf
23	p-p90RSK	Thr359/Ser363	MAPK	Ras-Raf
24	p-p90RSK	Ser380	MAPK	Ras-Raf
25	p-p90RSK	Thr573	MAPK	Ras-Raf
26	p-PAK1	Ser144	MAPK	Ras-Raf
27	p-PAK1	Ser199/204	MAPK	Ras-Raf
28	p-PAK1	Thr423	MAPK	Ras-Raf
29	p-PAK2	Ser20	MAPK	Ras-Raf
30	p-Raf-A	Ser299	MAPK	Ras-Raf
31	p-Raf-b	ser445	MAPK	Ras-Raf
32	p-Raf-c	Ser338	MAPK	Ras-Raf
33	p-Raf-c	Ser289/296/301	MAPK	Ras-Raf
34	p-Raf-c	Ser259	MAPK	Ras-Raf
35	p-RSK	Thr356/Ser360	MAPK	Ras-Raf
36	p-RSK2	Ser227	MAPK	PI3K-AKT-mTOR
37	p-EGF Receptor	Tyr1045	MAPK	RTK/TK
38	p-EGF Receptor	Tyr1068	MAPK	RTK/TK
39	p-EGF Receptor	Tyr992	MAPK	RTK/TK
40	p-PDGF Receptor-β	Thr1009	MAPK	RTK/TK
41	p-PDGF Receptor-β	Thr740	MAPK	RTK/TK
42	p-PDGF Receptor-β	Thr751	MAPK	RTK/TK
43	p-PDGF Receptor-β	Thr771	MAPK	RTK/TK
44	p-PDGF Receptor-β	Thr1021	MAPK	RTK/TK
45	p-ATF-2	Thr71	MAPK	SAPK/JNK
46	p-c-Jun	Ser63	MAPK	SAPK/JNK

47	p-c-Jun	Ser73	MAPK	SAPK/JNK
48	p-SAPK/JNK	Thr183/Y185	MAPK	SAPK/JNK
49	p-SAPK/JNK	Thr183/Tyr185	MAPK	SAPK/JNK
50	p-SEK1/MKK4	Thr261	MAPK	SAPK/JNK
51	p-TAK1	Thr184/187	MAPK	TGF-β
52	p-AMPKa	Thr172	mTOR	Glucose metabolism
53	p-IRS-1	Ser307	mTOR	Glucose metabolism
54	p-IRS-1	Ser612	mTOR	Glucose metabolism
55	p-IRS-1	Ser636/639	mTOR	Glucose metabolism
56	p-LKB1	Ser428	mTOR	Glucose metabolism
57	p-PKC(pan)βII	Ser660	mTOR	Phospholipase
58	p-PKCα/β	Thr638/641	mTOR	Phospholipase
59	p-4E-BP1	Thr70	mTOR	PI3K-AKT-mTOR
60	p-4E-BP1	Thr37/46	mTOR	PI3K-AKT-mTOR
61	p-4E-BP1	Ser65	mTOR	PI3K-AKT-mTOR
62	p70-S6 kinase	Thr389	mTOR	PI3K-AKT-mTOR
63	p-Akt	Thr308	mTOR	PI3K-AKT-mTOR
64	p-eEF2k	Ser366	mTOR	PI3K-AKT-mTOR
65	p-elF4B	Ser422	mTOR	PI3K-AKT-mTOR
66	p-elF4E	Ser209	mTOR	PI3K-AKT-mTOR
67	p-elF4G	Ser1108	mTOR	PI3K-AKT-mTOR
68	p-GSK-3a	Ser21	mTOR	PI3K-AKT-mTOR
69	p-GSK-3a/β	Ser21/9	mTOR	PI3K-AKT-mTOR
70	p-GSK-3β	Ser9	mTOR	PI3K-AKT-mTOR
71	Phospho-Akt	Ser473	mTOR	PI3K-AKT-mTOR
72	p-mTOR	Ser2448	mTOR	PI3K-AKT-mTOR
73	p-PDK1	Ser241	mTOR	PI3K-AKT-mTOR
74	p-PKD/PKCm	Ser744/748	mTOR	PI3K-AKT-mTOR
75	p-PKD/PKCm	Ser916	mTOR	PI3K-AKT-mTOR
76	p-PRAS40	Thr246	mTOR	PI3K-AKT-mTOR
77	p-PTEN	Ser380	mTOR	PI3K-AKT-mTOR
78	p-Raptor	Ser792	mTOR	PI3K-AKT-mTOR
79	p-S6Rb	Ser235/236	mTOR	PI3K-AKT-mTOR
80	p-S6Rb	Ser240/244	mTOR	PI3K-AKT-mTOR
81	p-Tuberin/TSC2	Ser939	mTOR	PI3K-AKT-mTOR
82	p-Tuberin/TSC2	Thr1462	mTOR	PI3K-AKT-mTOR
83	p-Tuberin/TSC2	Thr1571	mTOR	PI3K-AKT-mTOR

Abbreviations: CST, Cell Signaling Technology, Inc. (Danvers, MA)

[a]The MAPK and mTOR signaling components were selected based on KEGG pathway maps (http://www.genome.jp /kegg/kegg3a.html) and used for unsupervised hierarchical clustering analyses.

Supplementary Table S10. Fisher's exact test: Association of cancer types with activation status of the MAPK and mTOR signaling

	A[a]	B[b]	*P* value (fisher's exact test)
HCC	11	12	0.011
Ovarian Cancer	3	12	0.753
Gastric Cancer	3	12	0.753
Colon Cancer	2	7	1.000
Pancreatic Cancer	2	7	1.000
Osteosarcoma	0	8	0.109
Lung Cancer	3	5	0.416
Oral Cancer	0	7	0.185

[a,b] A and B indicate the subgroups shown in Supplementary Fig.2.

FULL PAPER

BJC

British Journal of Cancer (2015) 112, 704–713 | doi: 10.1038/bjc.2014.623

Keywords: copy number increase of *ACTN4*; locally advanced pancreatic cancer; chemotherapy; chemoradiotherapy; predictive biomarker

ACTN4 copy number increase as a predictive biomarker for chemoradiotherapy of locally advanced pancreatic cancer

T Watanabe[1,2], H Ueno[3], Y Watabe[1], N Hiraoka[4], C Morizane[3], J Itami[5], T Okusaka[3], N Miura[1], T Kakizaki[1], T Kakuya[1], M Kamita[1], A Tsuchida[2], Y Nagakawa[2], H Wilber[6], T Yamada[1] and K Honda*[,1]

[1]*Division of Chemotherapy and Clinical Research, National Cancer Center Research Institute, 5-1-1, Tsukiji, Chuo-ku, Tokyo 104-0045, Japan;* [2]*Department of Gastrointestinal and Pediatric Surgery, Tokyo Medical University, Tokyo 160-0023, Japan;* [3]*Hepatobiliary and Pancreatic Oncology Division, National Cancer Center Hospital, Tokyo 104-0045, Japan;* [4]*Division of Molecular Pathology, National Cancer Center Research Institute, Tokyo, 104-0045 Japan;* [5]*Division of Radiation Oncology, National Cancer Center Research Institute, Tokyo 104-0045, Japan and* [6]*Abnova, 9th Floor, No. 108, Jhouzih Street, Neihu District, Taipei City 114, Taiwan*

Background: Several clinical trials have compared chemotherapy alone and chemoradiotherapy (CRT) for locally advanced pancreatic cancer (LAPC) treatment. However, predictive biomarkers for optimal therapy of LAPC remain to be identified. We retrospectively estimated amplification of the *ACTN4* gene to determine its usefulness as a predictive biomarker for LAPC.

Methods: The copy number of *ACTN4* in 91 biopsy specimens of LAPC before treatment was evaluated using fluorescence *in situ* hybridisation (FISH).

Results: There were no statistically significant differences in overall survival (OS) or progression-free survival (PFS) of LAPC between patients treated with chemotherapy alone or with CRT. In a subgroup analysis of patients treated with CRT, patients with a copy number increase (CNI) of *ACTN4* had a worse prognosis of OS than those with a normal copy number (NCN) of *ACTN4* ($P=0.0005$, log-rank test). However, OS in the subgroup treated with chemotherapy alone was not significantly different between patients with a CNI and a NCN of *ACTN4*. In the patients with a NCN of *ACTN4*, the median survival time of PFS in CRT-treated patients was longer than that of patients treated with chemotherapy alone ($P=0.049$).

Conclusions: The copy number of *ACTN4* is a predictive biomarker for CRT of LAPC.

Despite progress in clinical cancer medicine in the fields of imaging technology, surgical management, therapeutic modalities and molecular-targeted therapy, the prognosis of pancreatic cancer has remained dismal. Every year in Japan, ~27 000 patients are diagnosed with pancreatic cancer, with almost the same number dying from this disease (Mayahara *et al*, 2012). Indeed, the 5-year overall survival (OS) rate of patients with pancreatic cancer is ⩽5% (Johung *et al*, 2012).

Locally advanced pancreatic cancer (LPAC) is defined as a surgically unresectable disease without detectable metastasis. Effective therapy for patients with LAPC is not only crucial for any hope of long-term survival, but also necessary for symptom management. Because survival rates for patients with LAPC are generally low, treatment recommendations often involve aggressive multimodal therapies (Savir *et al*, 2013). A multidisciplinary approach involving surgical oncologists, medical oncologists and radiation oncologists is strongly recommended for balanced discussion of management options (Pawlik *et al*, 2008; Katz *et al*, 2013; Mian *et al*, 2014).

At present, treatment options for LAPC include chemotherapy alone, induction chemotherapy followed by chemoradiotherapy (CRT) or definitive CRT. Numerous randomised trials have been

*Correspondence: Professor K Honda; E-mail: khonda@ncc.go.jp

Received 24 August 2014; revised 31 October 2014; accepted 25 November 2014; published online 20 January 2015

performed to compare the survival benefit between chemotherapy alone and CRT for LAPC (Chauffert *et al*, 2008; Loehrer *et al*, 2011). Nevertheless, as there are some contradictory results, the most effective treatment has not yet been defined for patients with LAPC (Savir *et al*, 2013; Mian *et al*, 2014). Radiotherapy focussed on the primary site does not have a direct impact on distant metastatic lesions and radiotherapy should therefore be limited to patients without metastases (Berger *et al*, 2008). If pancreatic cancer oncologists can accurately evaluate the occult distant metastasis before deciding the therapeutic strategy, they should be able to choose the optimal therapy for individual patients with LAPC. However, it is not yet possible to accurately detect micrometastatic lesions using imaging technology. Therefore, elucidation of biomarkers that can accurately evaluate metastatic potential from biopsy samples obtained from patients with LAPC is very important for deciding the best personalised therapeutic strategy from multimodal therapies.

In 1998, we identified actinin-4 (gene name *ACTN4*) as an actin-binding protein that is closely associated with cancer invasion and metastasis (Honda *et al*, 1998; Hayashida *et al*, 2005). Immunohistochemical analysis (IHC) showed that overexpression of the actinin-4 protein was significantly correlated with a poor prognosis for breast (Honda *et al*, 1998), pancreas (Kikuchi *et al*, 2008), ovary (Yamamoto *et al*, 2007, 2009, 2012) and lung cancer (Miyanaga *et al*, 2013; Noro *et al*, 2013).

We subsequently found that gene amplification of *ACTN4*, which is the gene name of the actinin-4 protein, is responsible for overexpression of the actinin-4 protein in a number of pancreatic cancer patients (Kikuchi *et al*, 2008). Using fluorescence *in situ* hybridisation (FISH), we then reported that gene amplification of *ACTN4* is a good biomarker for identification of patients with a poor prognosis for ovarian cancer (Yamamoto *et al*, 2009), salivary gland carcinoma (Watabe *et al*, 2014) and stage-I adenocarcinoma of the lung (Noro *et al*, 2013).

In this study, we retrospectively investigated the status of actinin-4 protein expression and *ACTN4* copy number in biopsy samples of LAPC patients. We confirmed the possibility that *ACTN4* copy number is useful as a predictive and prognostic biomarker of CRT for LAPC.

MATERIALS AND METHODS

Patients. A total of 91 patients who were diagnosed as having LAPC from May 2001 until December 2003 underwent chemotherapy alone or CRT at the National Cancer Center Central Hospital (Tokyo, Japan). All patients were diagnosed as adenocarcinoma of the pancreas by fine needle biopsy. This study was reviewed and approved by the institutional ethical committee and informed consent was obtained from the patients for this study.

At first diagnosis, multidetector computed tomography (CT) involving the chest and abdomen was performed for assessment of the local extension of the primary tumour, and for exclusion of distant metastasis. The CT-based criteria regarding tumour unresectability included enhancement or occlusion of the coeliac trunk, common hepatic artery, superior mesenteric artery or aorta (Ikeda *et al*, 2007; Mayahara *et al*, 2012).

Immunohistochemistry. Formalin-fixed, paraffin-embedded (FFPE) pathology blocks, which were made to diagnose the biopsy specimens, were cut into 4 μm-thick sections.

An anti-actinin-4 monoclonal antibody was established by our group (Miyanaga *et al*, 2013; Noro *et al*, 2013) (Abnova, Taipei, Taiwan). Immunostaining of actinin-4 was performed using the Ventana DABMap detection kit and an automated slide stainer (Discovery XT; Ventana Medical System, Tucson, AZ, USA) (Watabe *et al*, 2014). The immunohistochemical staining of actinin-4 was classified into two groups: positive and negative. Positive was defined as strong protein expression of actinin-4 in the cytoplasm and cell membranes of cancer cells. Negative was defined as no detection of actinin-4 protein in cancer cells or weak expression of actinin-4 in the cytoplasm or cell membrane of cancer cells (Figure 1). Two independent investigators (TW and YW) who had no clinical information about these cases evaluated the staining pattern.

Fluorescence *in situ* hybridisation. The FISH probes of the bacterial artificial chromosome (BAC) clone containing *ACTN4* were prepared by our group (Noro *et al*, 2013) (Abnova). The labelled BAC clone DNA was subjected to FISH as previously described. Sections that were cut from an FFPE biopsy block (4 μm thick) were hybridised with FISH probes at 37 °C for 48 h. The nuclei were counterstained with 4,6-duamidino-2-phenylindone. The number of fluorescence signals corresponding to the copy number of *ACTN4* in the nuclei of 20 interphase tumour cells was counted (TW and YW) (Watabe *et al*, 2014).

The FISH patterns were defined as described previously. Briefly, the biopsy samples were grouped as normal copy number (NCN) (two or fewer *ACTN4* signals in >90% of cells) and copy number increase (CNI) (four or more *ACTN4* signals in >10% of the tumour cells) (Figure 1) (Watabe *et al*, 2014).

Statistical analysis. Significant correlations were detected by using Fisher's exact test. Overall survival and progression-free survival (PFS) were measured as the period from first diagnosis to the event or last follow-up and were estimated by Kaplan–Meier analysis. Significant differences between curves of OS or PFS were assessed using the log-rank test. Univariate and multivariate analyses for death were performed using the Cox regression model. Data were analysed using the StatFlex statistical software package (version 6.0; Artiteck, Osaka, Japan) or the R-project (http://www.r-project.org/) (Honda *et al*, 2005, 2012; Noro *et al*, 2013).

RESULTS

Patient characteristics and survival benefit comparison between chemotherapy alone and CRT. In all, 34 patients with LAPC underwent chemotherapy alone. The regimens of chemotherapy alone comprised gemcitabine (GEM) alone ($n=29$), combination of GEM and erlotinib ($n=1$), combination of GEM and S-1 ($n=3$) or S-1 alone ($n=1$). A total of 57 patients with LAPC underwent CRT. The regimens of CRT comprised radiotherapy (RT) and 5-fluorouracil (5-FU) ($n=39$), RT and GEM ($n=10$) and RT and S-1 ($n=8$). The median age of patients and tumour size for all of the cases was 63.0 years and 37.4 mm, respectively. Statistical significances of patient characteristics with respect to age, gender, Eastern Cooperative Oncology Group Performance Status (PS), tumour size, lymph node metastasis and location of tumours were calculated. No statistically significant differences were observed between any of these factors and chemotherapy alone or CRT (Table 1).

The statistical significance of differences between the benefit of chemotherapy alone and that of CRT for OS and PFS was also calculated. In the absence of biomarker selection, no statistically significant differences in survival benefits in terms of OS and PFS were found between patients treated with chemotherapy alone and those treated with CRT (Figure 2).

Prognostic impact of protein expression of actinin-4 in patients with LAPC. We previously showed that protein overexpression of actinin-4 is a prognostic biomarker for resectable invasive ductal adenocarcinoma of the pancreas (Kikuchi *et al*, 2007). We investigated the protein expression level of actinin-4 in LAPC by using IHC. The 91 patients with LAPC were classified into one

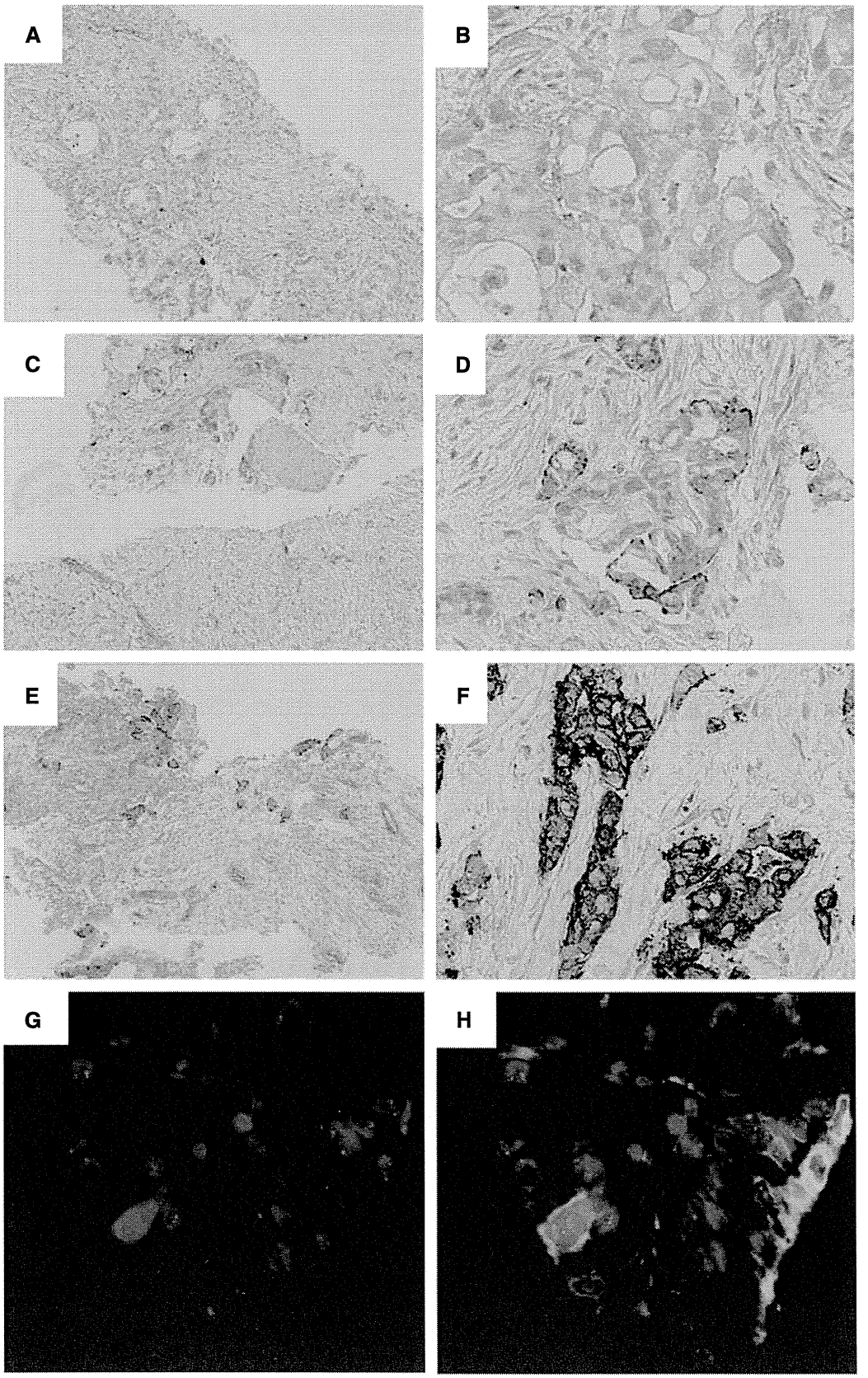

Figure 1. Immunohistochemical (IHC) and fluorescence *in situ* hybridisation (FISH) analyses of representative actinin-4 protein expression and *ACTN4* copy number, respectively, in LAPC biopsy specimens. (**A–F**) Immunohistochemical analysis of actinin-4 protein expression. Representative cases of no expression (**A**, **B**), weak expression (**C**, **D**) and strong expression (**E**, **F**) of actinin-4 protein in LAPC cells. (**A**), (**C**) and (**E**) are low-magnitude images. (**B**), (**D**) and (**F**) are high-magnitude images of regions of (**A**), (**C**) and (**E**), respectively. (**G**, **H**) Fluorescence *in situ* hybridisation analysis of representative cases with a copy number increase (CNI) in *ACTN4*.

Table 1. Baseline patient characteristics

	Total		CRT		CT		
Characteristic	**Number**	**%**	**Number**	**%**	**Number**	**%**	***P*-value***
Median age, years (63.0)							0.0501
<63.0	45	49.5	32	56.1	13	38.2	
⩾63.0	46	50.5	25	43.9	21	61.8	
Gender							1
Male	53	58.2	33	57.9	20	58.8	
Female	38	41.8	24	42.1	14	41.2	
PS							0.2681
0	26	28.6	17	29.8	9	26.5	
1	63	69.2	40	70.2	23	67.6	
2	2	2.2	0	0.0	2	5.9	
Median tumour size, mm (37.4)							0.3862
<37.4 mm	44	48.4	14	41.2	30	52.6	
⩾37.4 mm	47	51.6	20	58.8	27	47.4	
Lymph node metastasis							1
Negative	64	70.3	40	70.2	24	70.6	
Positive	27	29.7	17	29.8	10	29.4	
Location of the tumour							0.0501
Head of pancreas	43	47.3	22	38.6	21	61.8	
Body or tail of pancreas	48	52.7	35	61.4	13	38.2	
CA19-9							
<1000 U ml^{-1}	62	68.1	39	68.4	23	67.6	1
⩾1000 U ml^{-1}	29	31.9	18	31.6	11	32.4	

Abbreviations: CRT = chemoradiotherapy; CT = chemotherapy; PS = Eastern Cooperative Oncology Group Performance Status. **P*-value: Fisher's exact test (two sided).

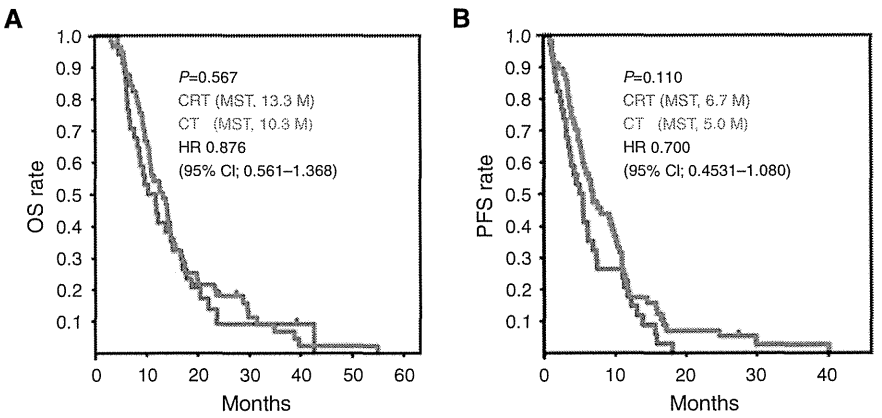

Figure 2. Kaplan–Meier analyses of overall survival (OS) and progression-free survival (PFS) in all locally advanced pancreatic cancer (LAPC) cases. The survival curves of all LAPC patients treated with chemotherapy alone (CT, blue lines) or with chemoradiotherapy (CRT, red lines) are shown. Statistically significant differences in OS (**A**) and PFS (**B**) were calculated using a log-rank test. Median survival time (MST) is shown in months (M). The clinical benefit of CT *vs* CRT was calculated by univariate Cox regression analysis (hazard ratio (HR) and 95% confidence interval (95% CI)). The y axis is the rate of OS or PFS, and the x axis is the time after first diagnosis (months).

of two groups based on actinin-4 protein expression; positive (66 patients, 72.5%) and negative (25 patients, 27.5%). We investigated correlations between protein expression of actinin-4 and the following patient characteristics: age, gender, PS, size of tumour, lymph node metastasis and treatment strategy (chemotherapy alone or CRT). Protein expression of actinin-4 was statistically correlated with tumour location ($P=0.0379$; Table 2).

We determined whether protein expression of actinin-4 provided benefit for OS to patients with LAPC by comparing the OS of cases of LAPC with and without actinin-4 expression (total, $n=91$). No statistically significant difference in OS between actinin-4 protein-positive and -negative cases was found ($P=0.116$, log-rank test; Figure 3A). However, although a statistical significance was not found by Kaplan–Meier analysis, the median survival time (MST) of OS of cases positive for acitinin-4 protein was 10.9 months, which was shorter than the MST of the negative cases (14.8 months) by 3.9 months (Figure 3A).

Determination of the copy number of *ACTN4* by FISH, and prognostic impact of copy number of *ACTN4* for LAPC. It is known that gene amplification of *ACTN4* is responsible for

Table 2. Association of protein expression of actinin-4 and copy number increase in *ACTN4* with clinicopathological characteristics of locally advanced pancreatic cancer

	Actinin-4 IHC					*ACTN4* FISH				
Characteristic	**Positive**	**%**	**Negative**	**%**	***P*-value***	**Positive**	**%**	**Negative**	**%**	***P*-value***
Median age, years (63.0)					0.159					0.41
<63.0	36	54.5	9	36.0		9	60.0	36	47.4	
⩾63.0	30	45.5	16	64.0		6	40.0	40	52.6	
Gender					0.6348					**0.02**
Male	37	56.1	16	64.0		13	86.7	40	52.6	
Female	29	43.9	9	36.0		2	13.3	36	47.4	
PS					0.3506					0.679
0	21	31.8	5	20.0		3	20.0	23	30.3	
1	44	66.7	19	76.0		12	80.0	51	67.1	
2	1	1.5	1	4.0		0	0.0	2	2.6	
Tumour size					0.8647					1
<37.4 mm	33	50.0	12	48.0		7	46.7	38	50.0	
⩾37.4 mm	33	50.0	13	52.0		8	53.3	38	50.0	
Lymph node metastasis					0.4478					0.059
Negative	48	72.7	16	64.0		7	46.7	57	75.0	
Positive	18	27.3	9	36.0		8	53.3	19	25.0	
Location of the tumour					**0.0379**					0.156
Head of pancreas	31	47.0	18	72.0		10	66.7	33	43.4	
Body or tail of pancreas	35	53.0	7	28.0		5	33.3	43	56.6	
CA19-9					0.451					0.227
$<1000\ U\ ml^{-1}$	43	65.2	19	76.0		8	53.3	54	71.1	
$\geqslant 1000\ U\ ml^{-1}$	23	34.8	6	24.0		7	46.7	22	28.9	
Therapy					1					1
CT	25	37.9	9	36.0		6	40.0	28	36.8	
CRT	41	62.1	16	64.0		9	60.0	48	63.2	

Abbreviations: *ACTN4* = *actinin-4*; CRT = chemoradiotherapy; CT = chemotherapy; FISH = fluorescence *in situ* hybridisation; IHC = immunohistochemistry; PS = Eastern Cooperative Oncology Group Performance Status. **P*-value: Fisher's exact test (two sided). Bold entries indicate statistically significance.

overexpression of actinin-4 protein in a number of patients with pancreatic cancer. In addition, gene amplification of *ACTN4* predicts a poorer prognosis than protein overexpression of actinin-4 in ovarian (Yamamoto *et al*, 2009), lung (Noro *et al*, 2013) and salivary gland cancer (Watabe *et al*, 2014). To evaluate the significance of *ACTN4* as a prognostic factor for LAPC, we determined the copy number of *ACTN4* in patients with LAPC by FISH. Of the 91 LAPC patients whom we examined, 76 patients were classified as NCN (83.5%) and 15 patients were classified as CNI (16.5%). Although only 1 of the 25 cases who were negative for actinin-4 protein (4.0%) had a CNI of *ACTN4*, 14 of the 66 cases who were actinin-4 protein positive (21.2%) had a CNI of *ACTN4* (Table 3). We also analysed association of the *ACTN4* copy number, as assessed by FISH analysis, with clinicopathological characteristics. There were statistically significant differences between gender and copy number of *ACTN4* ($P = 0.02$; Table 2).

When all cases of LAPC were considered, the difference in OS between cases with a CNI and those with NCN of *ACTN4* was statistically significant ($P = 0.0019$, log-rank test). The MST of OS in the cases with a CNI of *ACTN4* (8.7 months) was also significantly shorter than the MST of NCN cases (13.7 months) by 5 months ($P = 0.0019$; Figure 3B).

Prognostic impact of the serum level of CA19-9 in patients with LAPC. The serum level of CA19-9 has been reported to be a prognostic factor for patients with LAPC (Berger *et al*, 2008; Mayahara *et al*, 2012; Yang *et al*, 2013). We confirmed the usefulness of the serum level of CA19-9 as a prognostic factor for patients with LAPC in our study. The LAPC patients were classified into one of two groups: CA19-9 high expression ($\geqslant 1000\ U\ ml^{-1}$) and CA19-9 low–intermediate expression ($<1000\ U\ ml^{-1}$), as previously described (Mayahara *et al*, 2012). There was a statistically significant difference in OS between the CA19-9 high-expression group and the CA19-9 low–intermediate-expression group ($P = 0.0003$, log-rank test; Supplementary Figure 1). The MST of the CA19-9 high-expression group was 9.3 months, which was shorter than the MST of the CA19-9 low–intermediate-expression group (14.6 months) by 5.3 months.

Univariate analysis indicated that the risk factors for death of LAPC patients were: lymph node metastasis, serum level of CA19-9 (cutoff value; $1000\ U\ ml^{-1}$) and copy number status of *ACTN4*. The hazard ratios (HRs) for the death of patients with LAPC of lymph node metastasis, CA19-9 and a CNI of *ACTN4* were: 1.606 (95% confidence interval (CI); 1.008–2.560, $P = 0.0463$), 2.354 (95% CI; 1.479–3.761, $P = 0.0003$) and 2.531 (95% CI; 1.394–4.597, $P = 0.0023$), respectively. By multivariate analysis, the serum level of CA19-9 (HR; 2.325, 95% CI; 1.416–3.818, $P = 0.0009$) and a CNI of *ACTN4* (HR; 2.645, 95% CI; 1.439–4.861, $P = 0.0017$) were independent risk factors for the death of patients with LAPC. The HR of CNI of *ACTN4* (HR; 2.531) was slightly higher than that of the serum level of CA19-9 (HR; 2.354; Table 4).

Evaluation of OS in subgroup analyses of treatment strategy with copy number of *ACTN4*. A biomarker that can evaluate the potential for metastatic activity in tumour cells has the possibility of use as a predictive biomarker of CRT. It is known that *ACTN4* is an oncogene that is associated with cancer metastasis and cell invasion. In order to evaluate the benefit for OS based on the copy

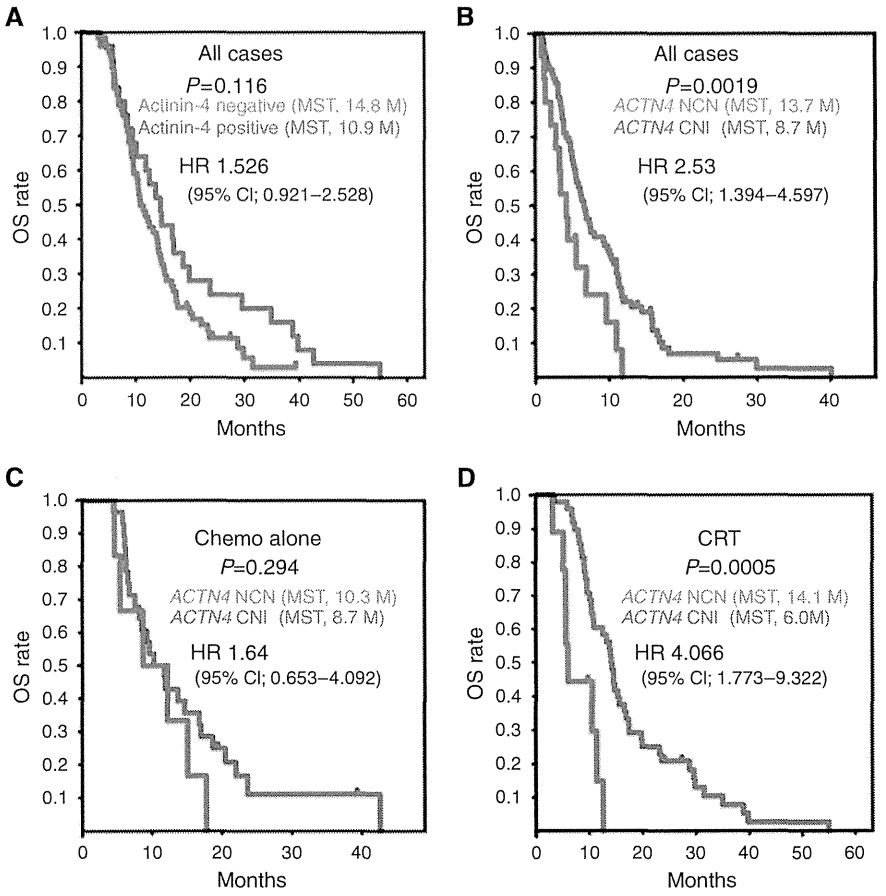

Figure 3. Kaplan–Meier analyses of survival relative to protein expression of actinin-4 and copy number of *ACTN4*. (**A**) Overall survival (OS) curves based on protein expression of actinin-4. The blue line represents patients with negative expression of actinin-4. The red line represents patients with positive expression of actinin-4. (**B–D**) The OS curves based on *ACTN4* copy number status in all cases ($n=91$) (**B**), in the subgroup treated with chemotherapy alone (Chemo alone, $n=34$) (**C**) and in the chemoradiotherapy (CRT)-treated subgroup ($n=57$) (**D**). The blue lines represent patients who were evaluated as normal copy number (NCN) of *ACTN4*. The red lines represent patients who were evaluated as copy number increase (CNI) of *ACTN4*. Statistical parameters were calculated as described for Figure 2. The y axis is the rate of OS, and the x axis is the time after first diagnosis (months).

Table 3. Statistical analysis of the association between the status of protein expression of actinin-4 and the copy number of *ACTN4*

	Copy number status of *ACTN4*			
Status of actinin-4 with IHC	**NCN (%)**	**CNI (%)**	**Total**	***P*-value***
Negative	24 (96.0)	1 (4.0)	25	**0.042**
Positive	52 (78.8)	14 (21.2)	66	
Total	76 (83.5)	15 (16.5)	91	

Abbreviations: *ACTN4* = *actinin-4*; CNI = copy number increase; IHC = immunohistochemistry; NCN = normal copy number. **P*-value: Fisher's exact test (one sided). Bold entry indicates statistically significance.

number status of *ACTN4* for each treatment strategy, the patients with LAPC were classified into one of two subgroups on the basis of treatment strategies: a chemotherapy-alone group and a CRT group. We then analysed the impact of the copy number status of *ACTN4* on OS of each subgroup. No statistical significance was observed between OS of patients with a NCN and with a CNI of *ACTN4* in the chemotherapy-alone subgroup ($P=0.294$, log-rank test). The MST of CNI and NCN of *ACTN4* patients was almost the same at 8.7 and 10.3 months, respectively (Figure 3C). Univariate Cox regression analysis indicated that the HR for death of CNI patients compared with NCN patients was 1.64 (95% CI; 0.653–4.092) in the chemotherapy-alone subgroup, and no statistically significant difference was found between CNI and NCN patients in the chemotherapy-alone subgroup ($P=0.291$).

In contrast, in the subgroup who underwent CRT, the OS of CNI of *ACTN4* patients was significantly worse than that of patients with a NCN ($P=0.0005$, log-rank test), and the MST of CNI of *ACTN4* patients (6.0 months) was definitely shorter than that of NCN of *ACTN4* patients (14.1 months; Figure 3D). Univariate Cox regression analysis of the CRT groups indicated that the HR for death of CNI patients compared with that for NCN patients was 4.066 (95% CI; 1.773–9.322), and the difference between CNI and NCN groups was statistically significant ($P=0.0009$). The HR for death in the comparison between CNI and NCN of *ACTN4* (4.066) patients in the CRT subgroup was higher than that of the HR in the comparison between the CNI and NCN of *ACTN4* patients in all 91 cases (HR; 2.531; Table 4).

We also calculated the prognostic impact of the serum level of CA19-9 in each subgroup of therapeutic strategy on OS. The OS of patients with high expression of CA19-9 was significantly worse than that of patients with low–intermediate expression of CA19-9 in both subgroups of the chemotherapy-alone group ($P=0.00218$, log-rank test; Supplementary Figure 2) and the CRT group ($P=0.0095$; Supplementary Figure 3).

Table 4. Univariate and multivariate Cox proportional hazard models to predict survival of patients with locally advanced pancreatic cancer receiving chemotherapy or chemoradiotherapy

	Univariate analysis			Multivariate analysis		
	HR	95% CI	*P*-value	HR	95% CI	*P*-value
Median age, years (63.0)						
<63.0/⩾63.0	0.959	0.624–1.474	0.8498			
Gender						
Male/female	0.802	0.519–1.249	0.334			
PS						
0/1 and 2	1.126	0.697–1.819	0.6270			
Median tumour size, mm (37.4)						
<37.4 mm/⩾37.4 mm	1.066	0.665–1.709	0.7902			
Lymph node metastasis						
Negative/positive	**1.606**	**1.008–2.560**	**0.0463**	1.199	0.7654–1.978	0.0740
Location of the tumour						
Head/body or tail of pancreas	0.764	0.492–1.185	0.2294			
CA19-9						
<1000/⩾1000 U ml^{-1}	**2.354**	**1.479–3.761**	**0.0003**	**2.325**	**1.416–3.818**	**0.0009**
Actinin-4 IHC						
Negative/positive	1.526	0.922–2.528	0.1004			
***ACTN4* FISH**						
NCN/CNI	**2.531**	**1.394–4.597**	**0.0023**	**2.645**	**1.439–4.861**	**0.0017**

Abbreviations: *ACTN4* = *actinin-4*; 95% CI = 95% confidence interval; CNI = copy number increase; FISH = fluorescence *in situ* hybridisation; HR = hazard ratio; IHC = immunohistochemistry; NCN = normal copy number; PS = Eastern Cooperative Oncology Group Performance Status. Bold entries indicate statistically significance.

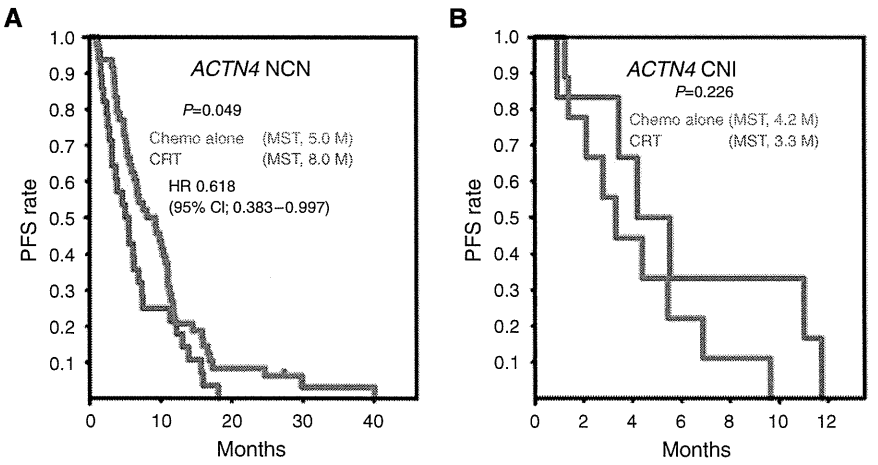

Figure 4. Kaplan–Meier analyses of progression-free survival (PFS) in CNI and NCN subgroups of *ACTN4*. The PFS curves of patients with a NCN of *ACTN4* (**A**) or a CNI of *ACTN4* (**B**), treated with chemotherapy alone (chemo alone, blue line) or with chemoradiotherapy (CRT, red line). The y axis is the rate of PFS and the x axis is the time after first diagnosis (months). Statistical parameters were calculated as described for Figure 2.

The benefit for PFS of CRT-treated patients who were selected by copy number status of *ACTN4*. We further examined the ability of *ACTN4* copy number to function as a predictive biomarker for CRT using subgroup analysis of the copy number status of *ACTN4*. We classified the patients into CNI and NCI subgroups of *ACTN4* and compared PFS in these CNI and NCI subgroups of *ACTN4* patients between the two arms of chemotherapy alone and CRT. Kaplan–Meier analysis indicated a statistically significant difference in the PFS of NCN patients in the chemotherapy-alone group compared with that of the CRT subgroup ($P = 0.049$; Figure 4A). The median PFS of the patients who were evaluated as NCN of *ACTN4* in the CRT subgroup was 8.0 months, whereas that for NCN of *ACTN4* patients in the chemotherapy-alone subgroup was 5.0 months. Thus, the median PFS of patients with NCN of *ACTN4* in the CRT subgroup was longer than that of patients with NCN of *ACTN4* in the chemotherapy-alone subgroup by 3 months. The HR for tumour progression of patients with NCN of *ACTN4* in the CRT subgroup compared with the chemotherapy-alone subgroup was 0.618 (95% CI; 0.383–0.997). No statistically significant difference in the PFS of patients with a CNI of *ACTN4* was noted between the chemotherapy-alone and the CRT subgroups ($P = 0.226$; Figure 4B). However, the MST of PFS in patients with a CNI of *ACTN4* in the chemotherapy-alone subgroup (4.2 months) was slightly longer (0.9 month longer) than that of patients with a CNI of *ACTN4* in the CRT subgroup (3.3 months). For both cohorts, there were no statistically significant differences in OS between the chemotherapy-alone and the CRT subgroups (data not shown).

DISCUSSION

In this study, we demonstrated that CNI of *ACTN4* is a predictive biomarker for the therapeutic strategy of LAPC. Although there have been a large number of studies and trials regarding the best chemotherapeutic strategy for extension of survival of patients with LAPC (Colucci *et al*, 2002; Huguet *et al*, 2007; Moore *et al*, 2007; Chauffert *et al*, 2008; Loehrer *et al*, 2011), the optimal therapy for patients with LAPC has not yet been decided upon. Clinical trials have reported contradictory results. Thus, the ECOG E4201, FFCD/SFRO and LAP07 phase III trials reported that the MST of OS in patients who received CRT was improved (Loehrer *et al*, 2011), decreased (Chauffert *et al*, 2008) or showed no statistically significant survival benefit compared with patients who received chemotherapy alone. The results of these studies suggest that there is a potential benefit to selecting appropriate patients for intensified treatment.

In order to select either chemotherapy or CRT as a treatment strategy, the metastatic potential of the tumour itself needs to be accurately evaluated. This is because radiotherapy can only exert a direct physicochemical effect on the tumour at the primary tumour site that is exposed to radiation, whereas chemotherapy can access both the primary tumour and distant metastasis. Therefore, patients with latent metastatic lesions, including lesions that cannot be detected using modern technology, should receive only strong chemotherapy, whereas patients who definitely have no distant metastatic lesions before initial treatment should receive CRT in order to exert sufficient physicochemical impact on the primary tumour site. Our finding that *ACTN4* copy number is a predictive marker for selection of therapy for LAPC should therefore prove valuable for optimisation of treatment strategy and help to provide the maximum personalised medicine for individual patients. Other predictive markers for treatment selection strategy have been suggested. Smad4 (Dpc4) is a tumour-suppressor gene involved in cell motility that is inactivated in 53% of pancreatic cancers. Prospective validation of smad4 expression in cytological specimens suggested that smad4 may be a predictive biomarker, and that analysis of smad4 levels may lead to personalised treatment strategies for patients with LAPC (Crane *et al*, 2011).

In the present paper we could not find any statistically significant difference in OS or PFS between LAPC patients who were treated with either chemotherapy alone or with CRT (Figure 2), again suggesting the need for a predictive marker for selection of patients for specific treatment. The potential predictive marker we considered was gene amplification of ACTN4.

The *ACTN4* gene encodes the actinin-4 protein, an actin-bundling protein that was isolated by our group in 1998 (Honda *et al*, 1998). Its protein overexpression is closely associated with cancer invasion and cell motility. Actinin-4 has one actin-binding domain at the N-terminus, and actinin-4 monomers can form a homodimer by binding in the opposite direction to form a dumbbell-shaped structure (Otey and Carpen, 2004). The actinin-4 homodimer can strongly bind F-actin and subsequently form bundling F-actin. Moreover, the bundling F-actin formed by actinin-4 makes strong contact with the cell membrane, following which cellular protrusions that are associated with cell motility are formed on the cell membrane (Welsch *et al*, 2009). The protein overexpression of actinin-4 in cancer cells stimulates dynamic remodelling of the actin cytoskeleton, and it is for this reason that actinin-4-overexpressing cancer cells have metastatic potential (Hayashida *et al*, 2005). Indeed, there are some reports that patients with cancers showing protein overexpression of actinin-4 have significantly worse OS than patients with cancers who are negative for actinin-4 (Honda *et al*, 1998; Yamamoto *et al*, 2007; Noro *et al*, 2013). Moreover, Kikuchi *et al* (2008) reported that protein overexpression of actinin-4 was a poor prognostic factor for invasive ductal adenocarcinoma of the pancreas. However, in the present study we could not find a statistically significant positive correlation between actinin-4 protein overexpression and poor prognosis. One difference between our present study and the previous study of Kikuchi *et al* (2008) was that in the latter study protein expression of actinin-4 was immunohistochemically evaluated using whole pathological sections that were obtained from surgical samples, whereas in the present study protein expression of actinin-4 was immunohistochemically evaluated using biopsy specimens of LAPC. In the study of Kikuchi *et al* (2008), the staining pattern of endothelial cells as an internal control was used to accurately evaluate the protein expression level of actinin-4 in tumour cells. However, accurate evaluation of the protein expression level of actinin-4 from biopsy specimens was more difficult than from whole pathological sections because the biopsy specimens did not always include endothelial cells. These technical problems may therefore explain the difference in the results of the two studies. One cause of protein overexpression of actinin-4 in cancer cells is amplification of the *ACTN4* gene (Kikuchi *et al*, 2008) and it has been reported that the CNI of *ACTN4* is a better prognostic predictor than protein expression of actinin-4 (Yamamoto *et al*, 2009; Noro *et al*, 2013; Watabe *et al*, 2014). We found a statistically significant difference in OS between patients with a CNI and those with a NCN, and patients with a CNI had a worse prognosis in terms of OS than NCN patients (Figure 3B). Furthermore, multivariate Cox regression analysis indicated that a CNI of *ACTN4* and high serum CA19-9 levels were independent prognostic factors for the death of patients, and that the HR of CNI of *ACTN4* was higher than that of high CA19-9 levels (Table 4). These data confirmed the usefulness of CA19-9 as a prognostic factor for LAPC and further suggested that *ACTN4* might be a prognostic factor for LAPC.

Subgroup analyses of CNI and NCN patients who were treated with chemotherapy alone or with CRT using FISH to calculate *ACTN4* copy number showed that whereas the copy number of *ACTN4* may be a predictive biomarker for CRT of LAPC, CA19-9 was not a predictive biomarker for either chemotherapy alone or CRT. Thus, there was no statistically significant difference in OS between CNI and NCN patients in the subgroup who were treated with chemotherapy alone (Figure 3C). However, in the subgroup of patients who were treated with CRT, the CNI patients with an MST of 14.1 months had a significantly longer survival time than NCN patients who had an MST of 6.0 months (Figure 3D). In contrast, serum CA19-9 levels showed statistically significant differences in terms of OS for both subgroups (Supplementary Figures 1–3).

Our data further confirmed the usefulness of *ACTN4* as a predictive biomarker for CRT in the study of the PFS of patients with LAPC who were classified into CNI and NCN of *ACTN4* groups and were then further classified into subgroups based on therapeutic strategies. We found a statistically significant difference in good prognosis of PFS between the NCN group treated with CRT (MST of PFS of 8.0 months) compared with the NCN group treated with chemotherapy alone (5.0 months; Figure 4A). Interestingly, although no statistically significant difference in PFS was found between the subgroups of CNI of *ACTN4* who were treated with chemotherapy alone or with CRT, the MST of PFS was the reverse of that seen in the NCN group, with the MST of chemotherapy alone being 4.2 months and that of CRT being shorter at 3.3 months. These data suggest that, when considering therapy for LAPC patients, patients with a NCN of *ACTN4* should at least undergo CRT (Figure 4B). However, no statistically significant difference in benefit in OS was noted in subgroup analysis of CNI and NCN of *ACTN4* groups. It was considered that the number of patients in the subgroup of *ACTN4* was too small to statistically prove the clinical benefit of chemotherapy alone in the subgroup with CNI of *ACTN4*.

In conclusion, we showed that the copy number of *ACTN4* is not only a prognostic biomarker, but also a candidate predictive biomarker for the decision regarding effective treatment strategy. Although this was a retrospective study, it suggested that patients without gene amplification of *ACTN4* should undergo CRT. Although it was concluded that *ACTN4* is a biomarker of potential metastasis, this does not necessarily contraindicate a potential function for *ACTN4* copy number as a predictive biomarker for CRT of LAPC. More detailed analyses, including a prospective study, should be carried out to prove this possibility.

ACKNOWLEDGEMENTS

This work was supported by a Grant-in Aid for Scientific Research (B) and a Challenging Exploratory Research from the Ministry of Education, Culture, Sports, Science and Technology (METX) of Japan (to KH) and the National Cancer Center Research and Development Fund (23-A-38, and 23-A-11; to KH).

CONFLICT OF INTEREST

The authors declare no conflict of interest.

REFERENCES

Berger AC, Garcia Jr. M, Hoffman JP, Regine WF, Abrams RA, Safran H, Konski A, Benson 3rd AB, MacDonald J, Willett CG (2008) Postresection CA 19-9 predicts overall survival in patients with pancreatic cancer treated with adjuvant chemoradiation: a prospective validation by RTOG 9704. *J Clin Oncol* **26**(36): 5918–5922.

Chauffert B, Mornex F, Bonnetain F, Rougier P, Mariette C, Bouche O, Bosset JF, Aparicio T, Mineur L, Azzedine A, Hammel P, Butel J, Stremsdoerfer N, Maingon P, Bedenne L (2008) Phase III trial comparing intensive induction chemoradiotherapy (60Gy, infusional 5-FU and intermittent cisplatin) followed by maintenance gemcitabine with gemcitabine alone for locally advanced unresectable pancreatic cancer. Definitive results of the 2000-01 FFCD/SFRO study. *Ann Oncol* **19**(9): 1592–1599.

Colucci G, Giuliani F, Gebbia V, Biglietto M, Rabitti P, Uomo G, Cigolari S, Testa A, Maiello E, Lopez M (2002) Gemcitabine alone or with cisplatin for the treatment of patients with locally advanced and/or metastatic pancreatic carcinoma: a prospective, randomized phase III study of the Gruppo Oncologia dell'Italia Meridionale. *Cancer* **94**(4): 902–910.

Crane CH, Varadhachary GR, Yordy JS, Staerkel GA, Javle MM, Safran H, Haque W, Hobbs BD, Krishnan S, Fleming JB, Das P, Lee JE, Abbruzzese JL, Wolff RA (2011) Phase II trial of cetuximab, gemcitabine, and oxaliplatin followed by chemoradiation with cetuximab for locally advanced (T4) pancreatic adenocarcinoma: correlation of Smad4(Dpc4) immunostaining with pattern of disease progression. *J Clin Oncol* **29**(22): 3037–3043.

Hayashida Y, Honda K, Idogawa M, Ino Y, Ono M, Tsuchida A, Aoki T, Hirohashi S, Yamada T (2005) E-cadherin regulates the association between beta-catenin and actinin-4. *Cancer Res* **65**(19): 8836–8845.

Honda K, Okusaka T, Felix K, Nakamori S, Sata N, Nagai H, Ioka T, Tsuchida A, Shimahara T, Shimahara M, Yasunami Y, Kuwabara H, Sakuma T, Otsuka Y, Ota N, Shitashige M, Kosuge T, Buchler MW, Yamada T (2012) Altered plasma apolipoprotein modifications in patients with pancreatic cancer: protein characterization and multi-institutional validation. *PLoS One* 7(10): e46908.

Honda K, Yamada T, Endo R, Ino Y, Gotoh M, Tsuda H, Yamada Y, Chiba H, Hirohashi S (1998) Actinin-4, a novel actin-bundling protein associated with cell motility and cancer invasion. *J Cell Biol* **140**(6): 1383–1393.

Honda K, Yamada T, Hayashida Y, Idogawa M, Sato S, Hasegawa F, Ino Y, Ono M, Hirohashi S (2005) Actinin-4 increases cell motility and promotes lymph node metastasis of colorectal cancer. *Gastroenterology* **128**(1): 51–62.

Huguet F, Andre T, Hammel P, Artru P, Balosso J, Selle F, Deniaud-Alexandre E, Ruszniewski P, Touboul E, Labianca R, de Gramont A, Louvet C (2007) Impact of chemoradiotherapy after disease control with chemotherapy in locally advanced pancreatic adenocarcinoma in GERCOR phase II and III studies. *J Clin Oncol* **25**(3): 326–331.

Ikeda M, Okusaka T, Ito Y, Ueno H, Morizane C, Furuse J, Ishii H, Kawashima M, Kagami Y, Ikeda H (2007) A phase I trial of S-1 with concurrent radiotherapy for locally advanced pancreatic cancer. *Br J Cancer* **96**(11): 1650–1655.

Johung K, Saif MW, Chang BW (2012) Treatment of locally advanced pancreatic cancer: the role of radiation therapy. *Int J Radiat Oncol Biol Phys* **82**(2): 508–518.

Katz MH, Marsh R, Herman JM, Shi Q, Collison E, Venook AP, Kindler HL, Alberts SR, Philip P, Lowy AM, Pisters PW, Posner MC, Berlin JD, Ahmad SA (2013) Borderline resectable pancreatic cancer: need for standardization and methods for optimal clinical trial design. *Ann Surg Oncol* **20**(8): 2787–2795.

Kikuchi S, Honda K, Handa Y, Kato H, Yamashita K, Umaki T, Shitashige M, Ono M, Tsuchida A, Aoki T, Hirohashi S, Yamada T (2007) Serum albumin-associated peptides of patients with uterine endometrial cancer. *Cancer Sci* **98**(6): 822–829.

Kikuchi S, Honda K, Tsuda H, Hiraoka N, Imoto I, Kosuge T, Umaki T, Onozato K, Shitashige M, Yamaguchi U, Ono M, Tsuchida A, Aoki T, Inazawa J, Hirohashi S, Yamada T (2008) Expression and gene amplification of actinin-4 in invasive ductal carcinoma of the pancreas. *Clin Cancer Res* **14**(17): 5348–5356.

Loehrer Sr. PJ, Feng Y, Cardenes H, Wagner L, Brell JM, Cella D, Flynn P, Ramanathan RK, Crane CH, Alberts SR, Benson 3rd AB (2011) Gemcitabine alone versus gemcitabine plus radiotherapy in patients with locally advanced pancreatic cancer: an Eastern Cooperative Oncology Group trial. *J Clin Oncol* **29**(31): 4105–4112.

Mayahara H, Ito Y, Morizane C, Ueno H, Okusaka T, Kondo S, Murakami N, Morota M, Sumi M, Itami J (2012) Salvage chemoradiotherapy after primary chemotherapy for locally advanced pancreatic cancer: a single-institution retrospective analysis. *BMC Cancer* **12**: 609.

Mian OY, Ram AN, Tuli R, Herman JM (2014) Management options in locally advanced pancreatic cancer. *Curr Oncol Rep* **16**(6): 388.

Miyanaga A, Honda K, Tsuta K, Masuda M, Yamaguchi U, Fujii G, Miyamoto A, Shinagawa S, Miura N, Tsuda H, Sakuma T, Asamura H, Gemma A, Yamada T (2013) Diagnostic and prognostic significance of the alternatively spliced ACTN4 variant in high-grade neuroendocrine pulmonary tumours. *Ann Oncol* **24**(1): 84–90.

Moore MJ, Goldstein D, Hamm J, Figer A, Hecht JR, Gallinger S, Au HJ, Murawa P, Walde D, Wolff RA, Campos D, Lim R, Ding K, Clark G, Voskoglou-Nomikos T, Ptasynski M, Parulekar W. National Cancer Institute of Canada Clinical Trials G (2007) Erlotinib plus gemcitabine compared with gemcitabine alone in patients with advanced pancreatic cancer: a phase III trial of the National Cancer Institute of Canada Clinical Trials Group. *J Clin Oncol* **25**(15): 1960–1966.

Noro R, Honda K, Tsuta K, Ishii G, Maeshima AM, Miura N, Furuta K, Shibata T, Tsuda H, Ochiai A, Sakuma T, Nishijima N, Gemma A, Asamura H, Nagai K, Yamada T (2013) Distinct outcome of stage I lung adenocarcinoma with ACTN4 cell motility gene amplification. *Ann Oncol* **24**(10): 2594–2600.

Otey CA, Carpen O (2004) Alpha-actinin revisited: a fresh look at an old player. *Cell Motil Cytoskeleton* **58**(2): 104–111.

Pawlik TM, Laheru D, Hruban RH, Coleman J, Wolfgang CL, Campbell K, Ali S, Fishman EK, Schulick RD, Herman JM. Johns Hopkins Multidisciplinary Pancreas Clinic T (2008) Evaluating the impact of a single-day multidisciplinary clinic on the management of pancreatic cancer. *Ann Surg Oncol* **15**(8): 2081–2088.

Savir G, Huber KE, Saif MW (2013) Locally advanced pancreatic cancer. Looking beyond traditional chemotherapy and radiation. *JOP* **14**(4): 337–339.

Watabe Y, Mori T, Yoshimoto S, Nomura T, Shibahara T, Yamada T, Honda K (2014) Copy number increase of ACTN4 is a prognostic indicator in salivary gland carcinoma. *Cancer Med* **3**(3): 613–622.

Welsch T, Keleg S, Bergmann F, Bauer S, Hinz U, Schmidt J (2009) Actinin-4 expression in primary and metastasized pancreatic ductal adenocarcinoma. *Pancreas* **38**(8): 968–976.

Yamamoto S, Tsuda H, Honda K, Kita T, Takano M, Tamai S, Inazawa J, Yamada T, Matsubara O (2007) Actinin-4 expression in ovarian cancer: a novel prognostic indicator independent of clinical stage and histological type. *Mod Pathol* **20**(12): 1278–1285.

Yamamoto S, Tsuda H, Honda K, Onozato K, Takano M, Tamai S, Imoto I, Inazawa J, Yamada T, Matsubara O (2009) Actinin-4 gene amplification in ovarian cancer: a candidate oncogene associated with poor patient prognosis and tumor chemoresistance. *Mod Pathol* **22**(4): 499–507.

Yamamoto S, Tsuda H, Honda K, Takano M, Tamai S, Imoto I, Inazawa J, Yamada T, Matsubara O (2012) ACTN4 gene amplification and actinin-4 protein overexpression drive tumour development and histological progression in a high-grade subset of ovarian clear-cell adenocarcinomas. *Histopathology* **60**(7): 1073–1083.

Yang GY, Malik NK, Chandrasekhar R, Ma WW, Flaherty L, Iyer R, Kuvshinoff B, Gibbs J, Wilding G, Warren G, May KS (2013) Change in CA 19-9 levels after chemoradiotherapy predicts survival in patients with locally advanced unresectable pancreatic cancer. *J Gastrointest Oncol* **4**(4): 361–369.

Supplementary Information accompanies this paper on British Journal of Cancer website (http://www.nature.com/bjc)

F-box protein FBXW7 inhibits cancer metastasis in a non-cell-autonomous manner

Kanae Yumimoto,[1] Sayuri Akiyoshi,[2] Hiroki Ueo,[2] Yasuaki Sagara,[3] Ichiro Onoyama,[1] Hiroaki Ueo,[4] Shinji Ohno,[5] Masaki Mori,[6] Koshi Mimori,[2] and Keiichi I. Nakayama[1]

[1]Department of Molecular and Cellular Biology, Medical Institute of Bioregulation, Kyushu University, Fukuoka, Japan. [2]Department of Surgery, Kyushu University Beppu Hospital, Beppu, Japan. [3]Sagara Hospital, Kagoshima, Japan. [4]Ueo Breast Surgical Hospital, Oita, Japan. [5]Clinical Research Institute, National Hospital Organization Kyushu Cancer Center, Fukuoka, Japan. [6]Department of Gastroenterological Surgery, Graduate School of Medicine, Osaka University, Suita, Japan.

The gene encoding F-box protein FBXW7 is frequently mutated in many human cancers. Although most previous studies have focused on the tumor-suppressive capacity of FBXW7 in tumor cells themselves, we determined that FBXW7 in the host microenvironment also suppresses cancer metastasis. Deletion of *Fbxw7* in murine BM-derived stromal cells induced accumulation of NOTCH and consequent transcriptional activation of *Ccl2*. FBXW7-deficient mice exhibited increased serum levels of the chemokine CCL2, which resulted in the recruitment of both monocytic myeloid-derived suppressor cells and macrophages, thereby promoting metastatic tumor growth. Administration of a CCL2 receptor antagonist blocked the enhancement of metastasis in FBXW7-deficient mice. Furthermore, in human breast cancer patients, *FBXW7* expression in peripheral blood was associated with serum CCL2 concentration and disease prognosis. Together, these results suggest that FBXW7 antagonizes cancer development in not only a cell-autonomous manner, but also a non-cell-autonomous manner, and that modulation of the FBXW7/NOTCH/CCL2 axis may provide a potential approach to suppression of cancer metastasis.

Introduction

Metastasis is a major cause of death in cancer patients, and elucidation of the genes and mechanisms that underlie this process is expected to provide a basis for the development of new cancer treatments. Such mechanisms have remained poorly understood because of the complexity of metastasis, which includes detachment of cancer cells from a primary tumor followed by their invasion into surrounding tissue, entry into the circulatory system, and invasion and proliferation in distant organs. In addition to the genomic variation among malignant tumor cells, recent research has focused on the relationship between cancer and the host environment. BM-derived cells (BMDCs) — including T cells (1), B cells (2), granulocytic and monocytic myeloid-derived suppressor cells (G-MDSCs and Mo-MDSCs, respectively) (3–6), macrophages (7–10), BM-derived stromal cells (BMSCs) (11, 12), hematopoietic progenitor cells (HPCs) (13), and endothelial progenitor cells (EPCs) (14) — play pivotal roles in promoting metastasis, including facilitation of tumor cell growth and invasion as well as of angiogenesis (15).

Tumor cells and surrounding stromal cells secrete various growth factors, cytokines, and chemokines that promote cancer development (16, 17). Chemokines promote tumor development and progression in addition to recruiting immune cells to tumor sites. The chemokine CCL2 (also known as monocyte chemoattractant protein–1 [MCP-1]) regulates the recruitment of monocytes, macrophages, and other inflammatory cells to sites of inflammation through interaction with its receptor, CCR2 (18). CCL2 also contributes to the recruitment of monocytes/macrophages to sites of pulmonary metastasis in mice with breast cancer and then promotes tumor outgrowth (19). Systemic administration of neutralizing antibodies against CCL2 in mouse cancer models has resulted in marked attenuation of tumor growth, reduction in tumor blood vessel density, and inhibition of metastasis (19–23).

FBXW7 (also known as Fbw7, Sel-10, hCdc4, or hAgo) is the F-box protein component of an Skp1–Cul1–F-box protein–type (SCF-type) ubiquitin ligase, in which it functions as a receptor responsible for substrate recognition. Most of the substrates of FBXW7 are growth promoters, including c-MYC (24, 25), NOTCH (26–28), cyclin E (29–31), c-JUN (32, 33), KLF5 (34, 35), and mTOR (36), and FBXW7 is therefore thought to serve as a tumor suppressor. Analysis of *FBXW7* in many primary human tumors revealed that approximately 6% of the tumors harbored mutations in this gene (37). Mutations were detected most frequently in cholangiocarcinoma (35%) and T cell acute lymphocytic leukemia (T-ALL; 31%). Notably, 43% of the identified mutations were found to be missense mutations that resulted in amino acid substitutions at key arginine residues (Arg^{465} and Arg^{479}) within the WD40 domain that are responsible for substrate recognition, which suggests that defective degradation of FBXW7 substrates leads to tumorigenesis.

Prior findings in genetic analyses of mice in which *Fbxw7* is conditionally deleted in various tissues collectively support a pivotal role for FBXW7 in suppression of tumorigenesis in vivo. Conditional inactivation of *Fbxw7* in the T cell lineage of mice induced the development of thymic lymphoma as a result of excessive c-MYC accumulation (38). More than half of BM-specific FBXW7-deficient mice developed T-ALL within 16 weeks, manifesting

Authorship note: Kanae Yumimoto and Sayuri Akiyoshi contributed equally to this work.
Conflict of interest: The authors have declared that no conflict of interest exists.
Submitted: August 29, 2014; **Accepted:** November 20, 2014.
Reference information: *J Clin Invest.* doi:10.1172/JCI78782.

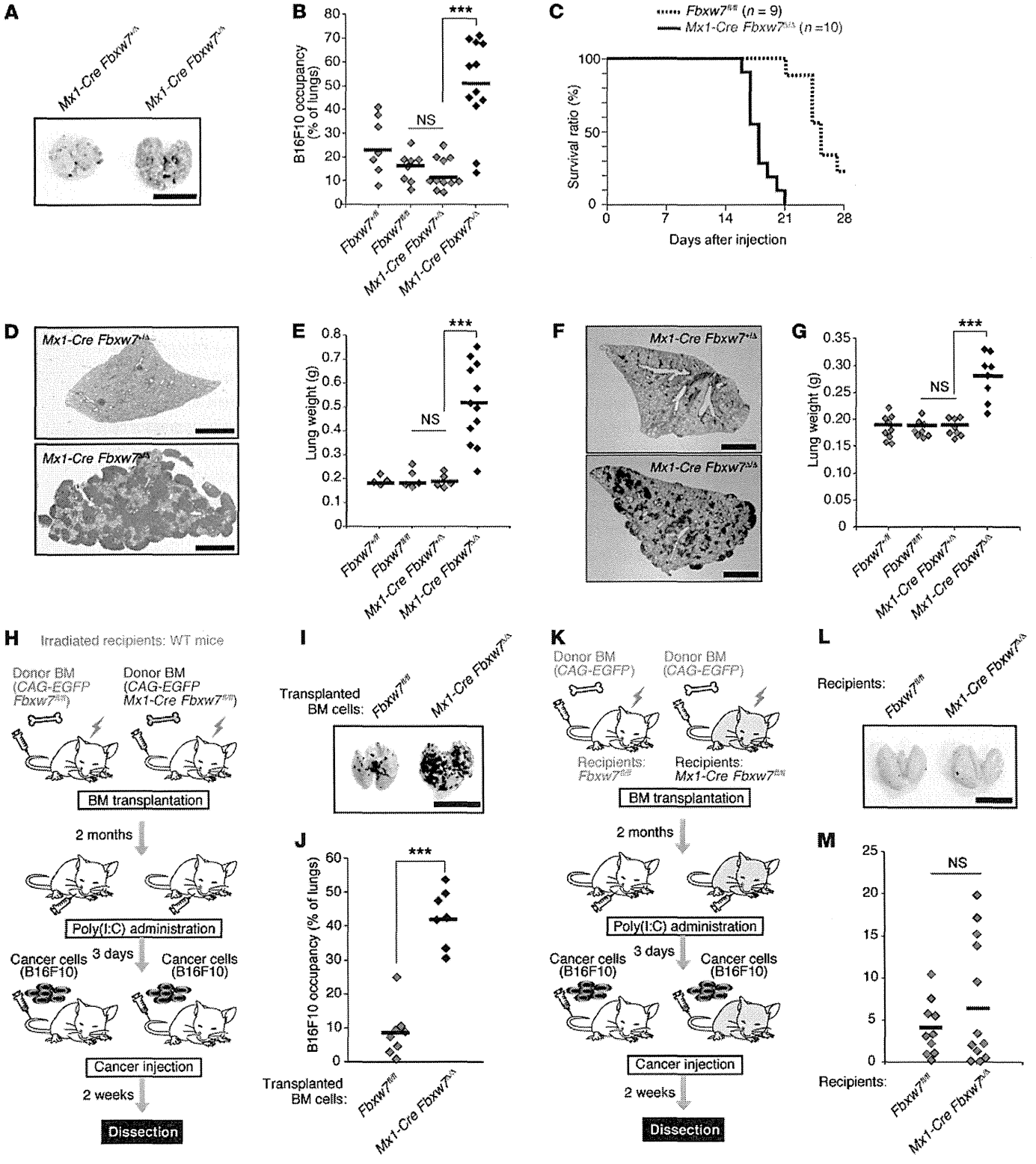

Figure 1. *Fbxw7* deletion in BM promotes cancer metastasis in an intravenous tumor cell transplantation model. (**A** and **B**) B16F10 cells were transplanted into *Fbxw7*$^{+/fl}$ (n = 7), *Fbxw7*$^{fl/fl}$ (n = 8), *Mx1-Cre Fbxw7*$^{+/\Delta}$ (n = 11), and *Mx1-Cre Fbxw7*$^{\Delta/\Delta}$ (n = 12) mice. The gross appearance of the lungs (**A**) and their occupancy by tumor colonies (**B**) were examined. Horizontal bars in **B** indicate mean values. (**C**) Kaplan-Meier survival curves for *Fbxw7*$^{fl/fl}$ (n = 9) and *Mx1-Cre Fbxw7*$^{\Delta/\Delta}$ (n = 10) mice after injection of B16F10 cells. (**D** and **E**) LLC cells were transplanted into *Fbxw7*$^{+/fl}$ (n = 4), *Fbxw7*$^{fl/fl}$ (n = 5), *Mx1-Cre Fbxw7*$^{+/\Delta}$ (n = 5), and *Mx1-Cre Fbxw7*$^{\Delta/\Delta}$ (n = 12) mice. (**F** and **G**) B16F1 cells were transplanted into *Fbxw7*$^{+/fl}$ (n = 9), *Fbxw7*$^{fl/fl}$ (n = 8), *Mx1-Cre Fbxw7*$^{+/\Delta}$ (n = 8), and *Mx1-Cre Fbxw7*$^{\Delta/\Delta}$ (n = 8) mice. Lungs were subjected to H&E staining (**D** and **F**), and their gross weight was determined (**E** and **G**). (**H**–**J**) Metastasis assays performed in WT mice reconstituted with *CAG-EGFP Fbxw7*$^{fl/fl}$ (n = 8) or *CAG-EGFP Mx1-Cre Fbxw7*$^{\Delta/\Delta}$ (n = 7) donor BM. (**K**–**M**) Metastasis assays performed in *Fbxw7*$^{fl/fl}$ (n = 10) or *Mx1-Cre Fbxw7*$^{\Delta/\Delta}$ (n = 12) mice reconstituted with WT donor BM. Schematic representation (**H** and **K**), gross appearance of the lungs (**I** and **L**), and their occupancy by tumor colonies (**J** and **M**) are shown. Scale bars: 10 mm (**A**, **I**, and **L**); 2 mm (**D** and **F**). Horizontal bars in **B**, **E**, **G**, **J**, and **M** indicate means. ***$P < 0.001$, 1-way ANOVA and Bonferroni test (**B**, **E**, and **G**) or 2-tailed Student's t test (**J**).

marked accumulation of NOTCH1 and c-MYC proteins (39, 40). FBXW7-null mice harboring a mutation in the adenomatous polyposis coli (*Apc*) gene (*Fbxw7*$^{\Delta/\Delta}$ *Apc*$^{min/+}$ mice) showed an increase in both number and size of intestinal tumors, and a consequently reduced survival rate, compared with *Apc*$^{min/+}$ mice (41). These various observations thus suggest that FBXW7 is a potent tumor suppressor in mice as well as in humans.

In the present study, we show that FBXW7 expression in the host environment is a key determinant of cancer metastasis. Metastasis was found to be enhanced in mice lacking FBXW7 in BM compared with control mice. We characterized the mechanism underlying this enhancement of metastasis: deletion of *Fbxw7* resulted in NOTCH accumulation and consequent activation of *Ccl2* gene transcription in BMSCs. The increased production of CCL2 by these cells likely promoted the formation of metastatic niches through recruitment of Mo-MDSC and macrophages. Inhibition of CCL2/CCR2 signaling reduced the frequency of metastasis in the FBXW7-deficient mice. Our results thus suggest that the FBXW7/NOTCH/CCL2 pathway plays a central role in the regulation of cancer metastasis.

Results

Deletion of Fbxw7 in BM promotes cancer metastasis in mice. Most studies of FBXW7 have focused on its functions in tumor cells (42–44); little is known regarding the role of this protein in the host microenvironment with respect to tumor development. To investigate the role of FBXW7 in the host microenvironment, we transferred B16F10 melanoma cells into the tail vein of *Mx1-Cre Fbxw7*$^{fl/fl}$ mice that had been injected with polyinosinic:polycytidylic acid [poly(I:C)] to delete floxed *Fbxw7* alleles selectively in BM (referred to hereafter as *Mx1-Cre Fbxw7*$^{\Delta/\Delta}$ mice). The frequency of metastasis of the melanoma cells to the lungs was markedly increased in *Mx1-Cre Fbxw7*$^{\Delta/\Delta}$ versus control mice (Figure 1, A and B), and this increased metastasis was accompanied by earlier death of the *Mx1-Cre Fbxw7*$^{\Delta/\Delta}$ mice (Figure 1C). Similar results were obtained when Lewis lung carcinoma (LLC) cells (Figure 1, D and E, and Supplemental Figure 1, A–C; supplemental material available online with this article; doi:10.1172/JCI78782DS1) or low–metastatic potential B16F1 melanoma cells (Figure 1, F and G, and Supplemental Figure 1, D–F) were injected into the tail vein of these mice. Thus, the level of FBXW7 in BM represents a key determinant of cancer metastasis in mice.

To examine whether ablation of *Fbxw7* specifically in BM was indeed responsible for the enhanced metastasis in *Mx1-Cre Fbxw7*$^{\Delta/\Delta}$ mice, we transplanted BM cells from *Mx1-Cre Fbxw7*$^{fl/fl}$ or control *Fbxw7*$^{fl/fl}$ mice that also harbor a transgene for enhanced green fluorescent protein (*EGFP*) under the control of the *CAG* promoter into irradiated C57BL/6 mice (Figure 1H). The recipient mice were subsequently injected with poly(I:C) to delete floxed alleles of *Fbxw7*; 3 days after injection, B16F10 or LLC cancer cells were transferred to these mice. Metastasis to the lungs was more pronounced in mice receiving *CAG-EGFP Mx1-Cre Fbxw7*$^{fl/fl}$ BM cells than in those receiving the control cells (Figure 1, I and J, and Supplemental Figure 1, G and H). In contrast, a reciprocal experiment revealed no such enhancement of metastasis in *Mx1-Cre Fbxw7*$^{fl/fl}$ mice subjected to transplantation with BM from *CAG-EGFP* mice and injected with poly(I:C) (Figure 1, K–M). These results confirmed that the loss of FBXW7 in BM is indeed responsible for the increased frequency of metastasis observed in *Mx1-Cre Fbxw7*$^{\Delta/\Delta}$ mice.

We also examined metastatic tumor growth in control and *Mx1-Cre Fbxw7*$^{\Delta/\Delta}$ mice after orthotopic transplantation of E0771 mouse breast cancer cells. Primary tumor growth was promoted in FBXW7-deficient mice on days 17 and 20, albeit not at later time points (Figure 2, A and B). Metastasis to the lungs was markedly enhanced in the mutant mice (Figure 2, C and D). In addition to lung weight, the total tumor area, number of tumor nodules, and average area per nodule in the lungs were greater for *Mx1-Cre Fbxw7*$^{\Delta/\Delta}$ mice than controls (Figure 2, D–G). We next monitored the progression of metastatic tumors in this model. Whereas we did not detect any tumor cells in the lungs at 12 days after cell transplantation, metastasis of E0771 cells was apparent in both control and *Mx1-Cre Fbxw7*$^{\Delta/\Delta}$ mice at 16 days (Figure 2, H–J). The number of tumor nodules and the average area per nodule did not differ between genotypes at 16 days after transplantation, but were significantly greater in *Mx1-Cre Fbxw7*$^{\Delta/\Delta}$ mice than in controls at 20 days. Although a premetastatic niche was previously shown to be formed by clusters of BMDCs (13), we found that such EGFP$^+$ clusters were already present at day 0 (before E0771 cell transplantation) in the lungs of WT mice reconstituted with EGFP-labeled *Mx1-Cre Fbxw7*$^{\Delta/\Delta}$ or control BM cells (Supplemental Figure 2A). The number of these clusters did not change substantially with time after E0771 cell transplantation and did not differ between the genotypes (Supplemental Figure 2B). In contrast, the number of diffusely infiltrated BMDCs in the lungs was increased after tumor cell transplantation specifically in mice reconstituted with *Mx1-Cre Fbxw7*$^{\Delta/\Delta}$ BM cells (Supplemental Figure 2, A and C). Immunofluorescence analysis with antibodies against TCRβ (for T cells), B220 (for B cells), Ly6G (for G-MDSCs), Ly6C (for Mo-MDSCs), F4/80 (for monocytes/macrophages), fibroblast-specific protein (FSP; for stromal cells), MAC1 (for myeloid cells), c-KIT (for HPCs), and VE-cadherin (for EPCs) revealed that the number of Ly6C$^+$, F4/80$^+$, and MAC1$^+$ cells increased among tumor-surrounding BMDCs, whereas only B220$^+$ cells moderately increased in number among the nonsurrounding BMDCs (Figure 3, A–F, and Supplemental Figure 3, A–C). These results suggested that accumulation of Mo-MDSCs or of more differentiated macrophages might be responsible for the promotion of metastasis in *Mx1-Cre Fbxw7*$^{\Delta/\Delta}$ mice.

We also characterized cells in the peripheral blood of mice at various times from 2 days before to 32 days after tumor cell transplantation. The frequency of MAC1$^+$Ly6G$^-$Ly6C$^+$ Mo-MDSCs and MAC1$^+$F4/80$^+$CD115$^+$ monocytes/macrophages in peripheral blood increased in *Mx1-Cre Fbxw7*$^{\Delta/\Delta}$ versus control mice before tumor cell transplantation, whereas the frequency of MAC1$^+$Ly6G$^+$Ly6C$^+$ immature MDSCs did not differ between the genotypes at this time (Supplemental Figure 2, D–F). However, the frequency of these latter cells in peripheral blood increased transiently — to a greater extent in *Mx1-Cre Fbxw7*$^{\Delta/\Delta}$ mice than in control mice — between days 16 and 24. In contrast, the frequency of MAC1$^+$Ly6G$^-$Ly6C$^+$ Mo-MDSCs in BM did not differ between genotypes at day 0 or day 20 (Supplemental Figure 2, G and H). Collectively, these results suggested that the increased infiltration of BMDCs during the early phase of metastasis to the lungs in *Mx1-Cre Fbxw7*$^{\Delta/\Delta}$ mice might rep-